Inductance Characteristics of the High-Frequency Transformer in Dual Active Bridge Converters

Xinyang Li, Weican Huang, Bin Cui, and Xiaohua Jiang
Department of Electrical engineering
Tsinghua University
Beijing 100084, China
jiangxiaohua@mail.tsinghua.edu.cn

***Abstract*—The high-frequency transformer (HFT) is an important component of dual active bridge (DAB) converters to achieve galvanic isolation and bidirectional power transmission, which is widely utilized in renewable energy, distribution grids, railway traction and electric ships. However, the real characteristics of the HFT such as magnetic inductance, leakage inductance and stray capacitance would influence the operation conditions of power converters. This paper analyzes the inductance characteristics of the HFT, focusing on the variation of the leakage inductance. To evaluate the magnitude of the leakage inductance, HFT samples wounded by nanocrystalline cores under 600 V/10 kW with various winding structures and air gap positions are simulated by finite element analysis (FEA) and tested by experimental measurements. The results show that the leakage inductance with the concentric windings is negligibly small, whereas the leakage inductance with the separate windings is so much larger that is even within the range of the phase-shift inductance required in DAB converters. On the other hand, the influence of air gaps on the leakage inductance is not evident not only in the concentric windings but also in the separate windings. A DAB prototype of 600 V/10 kW is designed and established, where the HFT with the separate windings has a leakage inductance adjusted to the magnitude of the phase-shift inductance required. The measurement results validate the feasibility that the phase-shift inductance could be substituted by the leakage inductance of the HFT.**

Keywords—high-frequency transformer, leakage inductance, nanocrystalline, magnetic integration

I. Introduction

The dual active bridge (DAB) converter becomes a research focus as the key interface to achieve galvanic isolation and bidirectional power flow in DC power systems recently [1], with the increasing requirements of renewable energy [2], distribution grids [3], railway traction [4] and electric ships [5]. In DAB systems, the high-frequency transformer (HFT) is an important component for galvanic isolation. With the increase of the operating frequency of power converters and the availability of high frequency materials such as nanocrystalline, the weight and volume of the HFT could be reduced significantly. Nowadays, the relative permeability of nanocrystalline materials could be as high as 10000 to 30000, and the saturation flux density could reach above 1 T while the core loss keeps at a low level even with an operating frequency up to 100 kHz [6].

In the DAB topology, the leakage inductance of the HFT could contribute to the phase-shift inductance. [7] evaluates the leakage inductance of concentric windings by FEA, which could be reduced to less than 1 μH with interleaved windings. [8] and [9] presents analytical methods to calculate the leakage inductance respectively. [10] proposes an optimization design method of the HFT to minimize the stray parameters including leakage inductance. In [11], the leakage inductance of the HFT is utilized as the phase-shift inductance of DAB by integrating the required inductance into the transformer.

This paper analyzes the leakage inductance characteristics of nanocrystalline HFT under various winding structures and air gap positions. The leakage inductances of HFT samples of nanocrystalline cores under 600 V/10 kW are simulated by finite element analysis (FEA) and measured by the LCR meter. The influences of both winding structures and air gap positions on the leakage inductance are discussed.

To validate the analysis above, a DAB prototype of 600 V/10 kW is established and tested, where the HFT sample with the separate windings has a leakage inductance adjusted to the magnitude of the phase-shift inductance required.

II. Inductance Characteristics of HFT

The inductance parameters of HFT include leakage inductance L_s and magnetic inductance L_m. The magnetic inductance is mainly determined by the magnetic core parameters and the number of winding turns, which could be further adjusted by length of air gaps. The leakage inductance is mainly affected by winding structures and relative winding parameters. Thus, the value of leakage inductance is relatively complex to be evaluated, as the corresponding leakage energy distributes in space.

In order to evaluate the leakage inductances of the nanocrystalline HFT under various winding structures and air gap positions, 600 V/10 kW HFT samples based on the AMMET AM-NC-120 nanocrystalline core are analyzed. The parameters of the magnetic core are listed in Table I.

A 1/4 HFT FEA model is established in Maxwell according to the magnetic core configuration to calculate the inductances of the samples, among which two samples (separate windings without air gap and separate windings with air gaps inside) are measured by the LCR meter.

TABLE I. Parameters of the Magnetic Core

Symbol	Parameter	Value
f_s	Operating frequency	40 kHz
μ_r	Relative magnetic permeability	20800
B_m	Saturation flux density	1.25 T
A_e	Effective cross section area	349.6 mm^2
L_e	Equvilant path length	286.8 mm

This work was supported by the National Natural Science Foundation of China under Grant 51877114.

978-1-7281-3398-0/19/$31.00 ©2019 IEEE

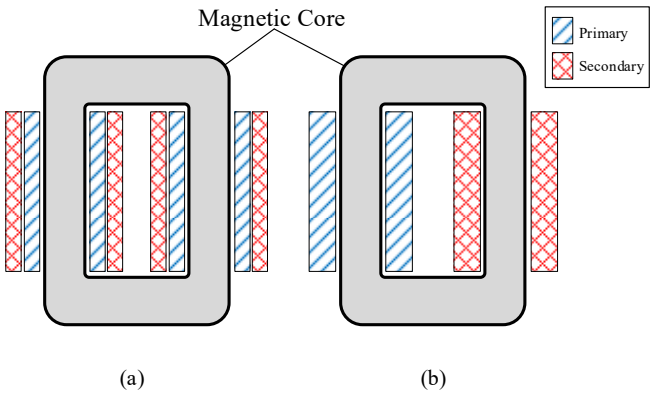

Fig. 1. Configurations of HFT with concentric windings and separate windings

A. Winding Sturcture

The configurations of the HFT with concentric windings and separate windings are shown as Fig. 1, which are widely utilized. And the factors which influence the leakage inductance of different structures are analyzed respectively.

- HFT with Concentric Windings

To evaluate the leakage inductance of the HFT, the short-circuit simulation is conducted. Fig. 2 shows the distribution of the energy in space of the HFT with concentric windings (N_1=N_2=40), from which the leakage inductance could be obtained by the integration of energy, with the result of 7.69 μH. It can be seen that the energy distributes in the space between the primary and secondary winding layers. Besides, the magnetic inductance of the HFT is calculated by the open-circuit simulation, with the result of 44.8 mH.

The leakage inductances and magnetic inductances with different numbers of winding turns are calculated by FEA while keeping the turns ratio n=1. Fig. 3 shows the variation of the inductances with the number of winding turns. It can be seen that the leakage inductance is negligibly small, while the magnetic inductance is very large due to the high relative permeability of nanocrystalline. As the number of winding turns varies from 15 to 40, the average operation magnetic flux density decreases from 0.715 T to 0.268 T, which is within the saturation flux density B_m.

To analyze the influence of the distance between the primary layer and the secondary layer, the leakage inductances and magnetic inductances with different distances l_d under N_1=N_2=40 are shown in Fig. 4. It can be seen that the leakage inductance increases linearly with the distance l_d, while the magnetic inductance keeps unchanged.

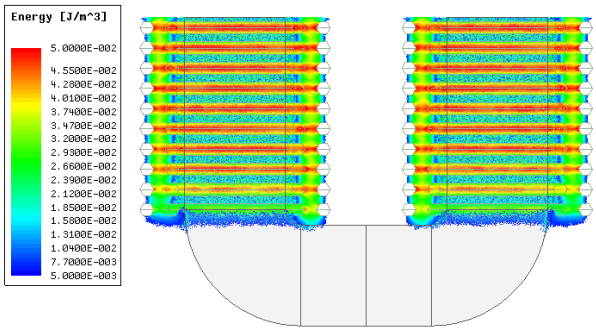

Fig. 2. Distribution of energy in space of HFT with concentric windings

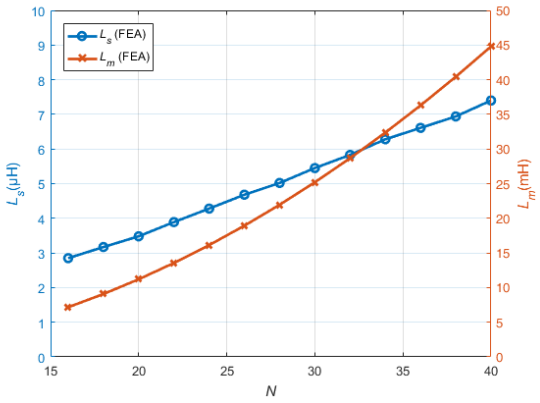

Fig. 3. Leakage inductance L_s and magnetic inductance L_m of HFT with concentric windings under different numbers of winding turns N

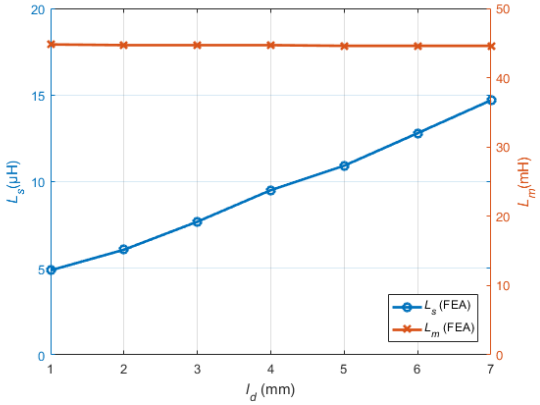

Fig. 4. Leakage inductance L_s and magnetic inductance L_m of HFT with concentric windings under different distances between primary and secondary layers l_d

- HFT with Separate Windings

For transformers with separate windings, Fig. 5 shows the distribution of the energy in space of the HFT (N_1=N_2=20). It can be seen that the energy distributes in the whole space, which is difficult to be calculated analytically. The simulation values of leakage inductance and magnetic inductance are 84.8 μH and 11.50 mH respectively.

Moreover, the energy mostly distributes near the winding ends, which is around the outer layers of the magnetic core. And the magnitude of leakage energy of the HFT with separate windings is much bigger than that with concentric windings.

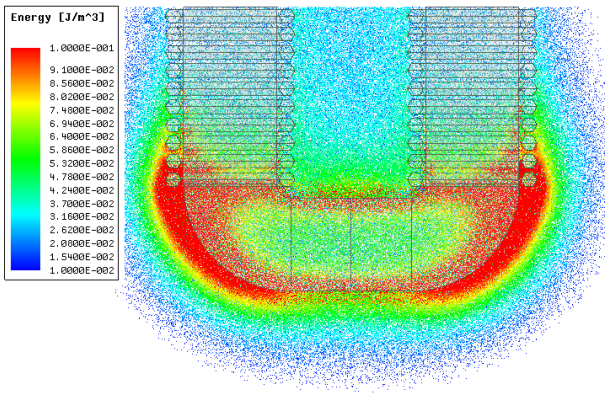

Fig. 5. Distribution of energy in space of HFT with separate windings

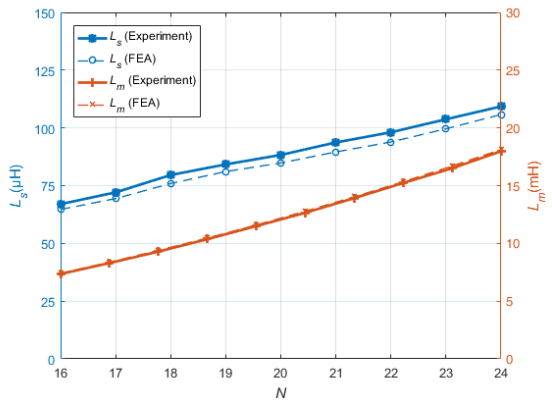

Fig. 6. Leakage inductance L_s and magnetic inductance L_m of the HFT with separate windings under different numbers of turns N

The leakage inductances and magnetic inductances of the HFT with separate windings under different numbers of winding turns are calculated by FEA while keeping the turns ratio n=1. Fig. 6 shows the variations of the inductances with the number of winding turns. It can be seen that the leakage inductance is significantly large, which is of the same magnitude as the phase-shift inductance of DAB.

Besides, from the comparison of FEA data and measurement results, the values of magnetic inductances are almost the same. The FEA values of leakage inductances are also close to the measurements, and the error of simulation is within 3.5%. Thus, the validity of the FEA model is verified.

Consequently, the leakage inductance of the HFT with separate windings could be adjusted by number of winding turns in a small range to the required value, while the average peak magnetic flux density of magnetic core varies little to guarantee the designed operation condition of the HFT.

B. Air Gap Positions

In order to adjust the magnetic inductance and deal with DC magnetic bias, the cut magnetic core is usually utilized. When the length of air gap is far less than the equivalent magnetic path length, the equivalent permeability of the cut core μ_e could be derived as

$$\mu_e = \frac{l_g + L_e}{\frac{l_g}{\mu_0} + \frac{L_e}{\mu_0 \mu_r}} \approx \frac{\mu_0 \mu_r}{1 + \mu_r \frac{l_g}{L_e}} \tag{1}$$

where μ_r is the relative permeability of the uncut magnetic core, and l_g is the length of the air gap.

Based on the parameters of magnetic core, the magnetic inductance L_m of the HFT with air gaps could be calculated as

$$L_m = \frac{N^2 \mu_e A_e}{L_e} \tag{2}$$

where A_e is the effective cross section area and L_e is the equivalent magnetic path length.

For leakage inductance characteristics of the HFT with cut cores, the position of air gaps would influence the magnetic circuit of leakage flux, and the typical positions at the limb and the yoke are shown as Fig. 7 (a) and Fig. 7 (b) respectively.

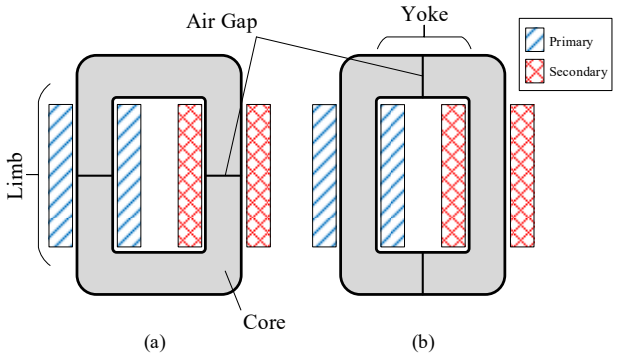

Fig. 7. Different positions of air gaps

The magnetic inductance and the leakage inductance of the HFT with different air gap positions are simulated under different lengths of air gaps and the same number of winding turns N_1=N_2=20. The FEA and experiment results are shown in Fig. 8.

It can be seen that the leakage inductance of the HFT with air gaps at the limb decreases linearly with the increase of air gap length l_g. In addition, the leakage inductance varies little compared with the magnetic inductance within a wide range of available lengths of air gaps. Thus, it is difficult to change the leakage inductance by adjusting the length of air gaps, whereas the magnetic inductance changes obviously. From the comparison of FEA data and measurement results, the error of simulation is within 2.2%.

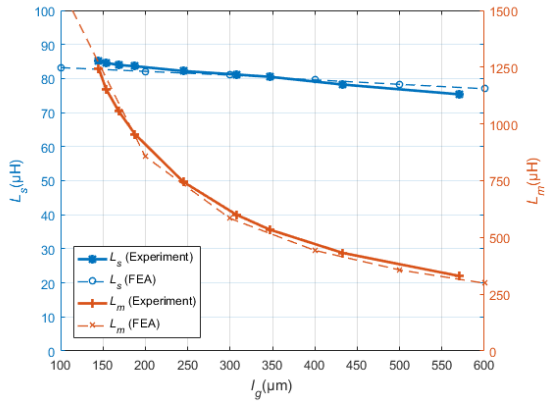

(a)

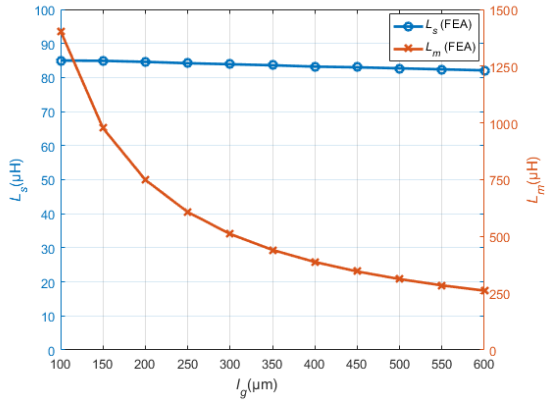

(b)

Fig. 8. Leakage inductance L_s and magnetic inductance L_m of the HFT with different air gap positions and lengths of air gaps l_g

Besides, the leakage inductance of the HFT with air gaps at the yoke varies quite little, where the magnetic inductance could be adjusted by different lengths of air gaps with negligible influences on the leakage inductance.

For the HFT with air gaps, the air gaps at the limb would affect the leakage inductance to a certain extent as they are within all the leakage magnetic circuits, whereas the air gaps at the yoke only affects a minor part of the leakage magnetic circuits, which has less influence on the leakage inductance.

Moreover, in order to keep the magnetic inductance L_m much larger than the leakage inductance L_s, it is necessary to increase the number of winding turns, which will lead to the increase of the leakage inductance. Therefore, the influence of air gaps needs to be considered in the HFT design process.

III. Magnetic Integration in DAB Converters

As the magnitude of the leakage inductance of the HFT with separate windings is in the range of the phase-shift inductance of DAB converters, the leakage inductance of the HFT might be utilized as the phase-shift inductance to achieve magnetic integration, which could further increase the power density.

The DAB topology with magnetic integration of the phase-shift inductance into the leakage inductance of the HFT is shown as Fig. 9. The circuit specifications are listed in Table II. An HFT sample with separate windings is designed and wounded according to the DAB specifications, shown in Fig. 10. The parameters of the HFT sample are listed in Table III, where the leakage inductance L_s is close to the required phase-shift inductance L_p.

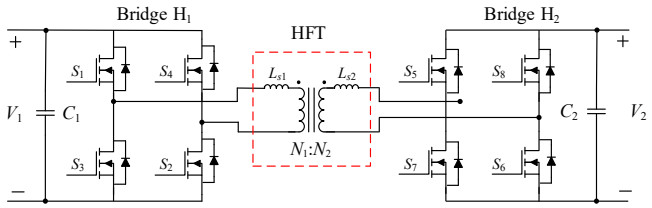

Fig. 9. DAB topology with intergrated phase-shift inductance

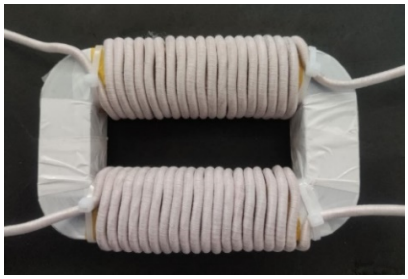

Fig. 10. Picture of the HFT Sample

TABLE II. Specifications of the DAB Prototype

Symbol	Parameter	Value
V_1	Input voltage	600 V
V_2	Output voltage	600 V
P	Rated power	10.0 kW
f_s	Switching frequency	40 kHz
L_p	Phase-shift inductance	84.4 μH
D	Rated duty ratio of phase shift	0.25

TABLE III. Parameters of the HFT Sample

Symbol	Parameter	Value
L_m	Magnetic inductance	11.27 mH
L_s	Leakage inductance	87.3 μH
N_1:N_2	Number of winding turns	20:20
f_s	Operating frequency	40 kHz
r_s	Winding resistance	0.0247 Ω
B_m	Average peak magnetic flux density	0.536 T

IV. Experimental Verification

The HFT sample is tested based on the DAB prototype. The input voltage V_1 and output voltage V_2 are both 600 V and the switching frequency is set at 40 kHz. The single-phase-shift (SPS) algorithm [1] is applied, and the duty ratio of phase shift between the input and output H bridges is set at 0.25. The input and output voltages and input current of the HFT are measured as shown in Fig. 11. It could be seen that the DAB prototype operates stably with the integrated phase-shift inductance.

The temperature distribution of the HFT is shown in Fig. 12, with the rated power of 10 kW being transmitted from the input side to the output side. It can be seen that the temperature of outer layers at the corners are higher than other parts of the HFT, and the heat is probably due to the leakage flux vertical to the tape-wounded nanocrystalline magnetic core which could result in high eddy current loss. [11]

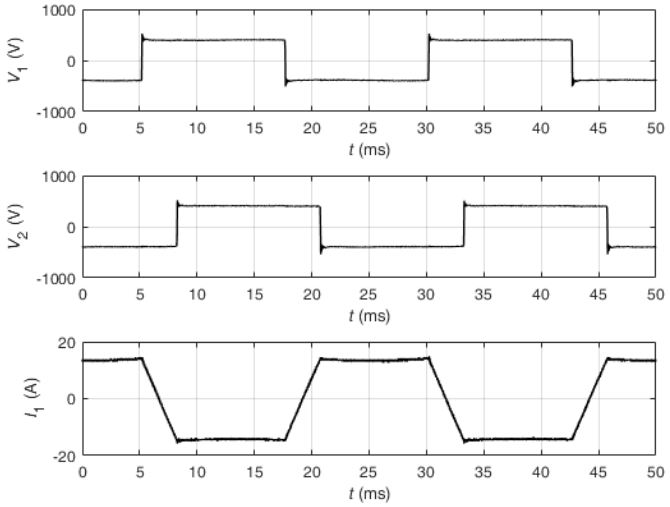

Fig. 11. Experimental waveforms of the HFT in DAB prototype

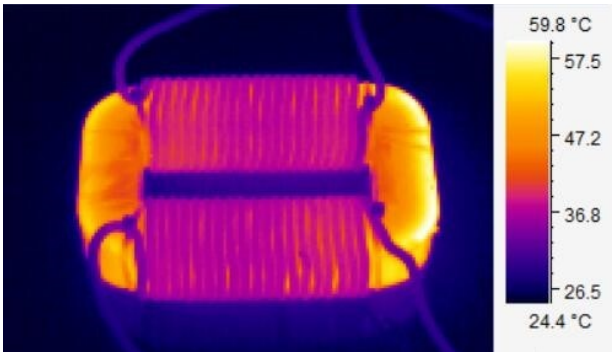

Fig. 12. Temperature distribution of the HFT sample

V. Conclusions

In this paper, the inductance characteristics of the HFT with different winding structures and air gap positions are simulated by FEA and measured by the LCR meter as validations. The results show that the leakage inductance with concentric windings is negligibly small. Whereas the leakage inductance with the separate windings is so much larger, which could be adjusted by number of winding turns in a small range to a required value. Moreover, the leakage inductance is even within the range of the phase-shift inductance required in DAB converters. On the other hand, the influence of air gaps on the leakage inductance is not evident not only in the concentric windings but also in the separate windings, therefore the leakage inductance could not be designed accordingly. A DAB prototype of 600 V/10 kW is designed and established, where the HFT sample with the separate windings has a leakage inductance adjusted to the magnitude of the phase-shift inductance required. The measurement results validate the feasibility that the phase-shift inductance could be substituted by the leakage inductance integrated in HFT.

For the HFT with separate windings, the temperature of outer layers of the tape-wounded nanocrystalline core is relative higher than other positions, which is probably due to the leakage flux vertical to the tapes resulting in high eddy current loss, which need to be considered in thermal design.

References

[1] B. Zhao, Q. Song, W. Liu and Y. Sun, "Overview of Dual-Active-Bridge Isolated Bidirectional DC–DC Converter for High-Frequency-Link Power-Conversion System," in IEEE Transactions on Power Electronics, vol. 29, no. 8, pp. 4091-4106, Aug. 2014.

[2] M. R. Islam, Y. Guo and J. Zhu, "A High-Frequency Link Multilevel Cascaded Medium-Voltage Converter for Direct Grid Integration of Renewable Energy Systems," in IEEE Transactions on Power Electronics, vol. 29, no. 8, pp. 4167-4182, Aug. 2014.

[3] X. She, A. Q. Huang and R. Burgos, "Review of Solid-State Transformer Technologies and Their Application in Power Distribution Systems," in IEEE Journal of Emerging and Selected Topics in Power Electronics, vol. 1, no. 3, pp. 186-198, Sept. 2013.

[4] Y. Chen, S. Zhao, Z. Li, X. Wei and Y. Kang, "Modeling and Control of the Isolated DC–DC Modular Multilevel Converter for Electric Ship Medium Voltage Direct Current Power System," in IEEE Journal of Emerging and Selected Topics in Power Electronics, vol. 5, no. 1, pp. 124-139, March 2017.

[5] C. Zhao et al., "Power Electronic Traction Transformer—Medium Voltage Prototype," in IEEE Transactions on Industrial Electronics, vol. 61, no. 7, pp. 3257-3268, July 2014.

[6] W. Shen, F. Wang, D. Boroyevich and C. W. Tipton, "Loss Characterization and Calculation of Nanocrystalline Cores for High-Frequency Magnetics Applications," in IEEE Transactions on Power Electronics, vol. 23, no. 1, pp. 475-484, Jan. 2008.

[7] Z. Ouyang, J. Zhang and W. G. Hurley, "Calculation of Leakage Inductance for High-Frequency Transformers," in IEEE Transactions on Power Electronics, vol. 30, no. 10, pp. 5769-5775, Oct. 2015.

[8] M. A. Bahmani, T. Thiringer and M. Kharezy, "Design Methodology and Optimization of a Medium-Frequency Transformer for High-Power DC–DC Applications," in IEEE Transactions on Industry Applications, vol. 52, no. 5, pp. 4225-4233, Sept.-Oct. 2016.

[9] M. Mogorovic and D. Dujic, "Medium frequency transformer leakage inductance modeling and experimental verification," 2017 IEEE Energy Conversion Congress and Exposition (ECCE), Cincinnati, OH, 2017, pp. 419-424.

[10] M. Mogorovic and D. Dujic, "Sensitivity Analysis of Medium-Frequency Transformer Designs for Solid-State Transformers," in IEEE Transactions on Power Electronics, vol. 34, no. 9, pp. 8356-8367, Sept. 2019.

[11] B. Cougo and J. W. Kolar, "Integration of Leakage Inductance in Tape Wound Core Transformers for Dual Active Bridge Converters," 2012 7th International Conference on Integrated Power Electronics Systems (CIPS), Nuremberg, 2012, pp. 1-6.